Acta Mech. Sin. (2011) 27(5):823–832
DOI 10.1007/s10409-011-0487-z

RESEARCH PAPER

Stabilization control of a hovering model insect: lateral motion

Yan-Lai Zhang · Mao Sun

Received: 22 March 2010 / Revised: 31 August 2010 / Accepted: 29 September 2010

Abstract Our previous study shows that the lateral disturbance motion of a model drone fly does not have inherent stability (passive stability), because of the existence of an unstable divergence mode. But drone flies are observed to fly stably. Constantly active control must be applied to stabilize the flight. In this study, we investigate the lateral stabilization control of the model drone fly. The method of computational fluid dynamics is used to compute the lateral control derivatives and the techniques of eigenvalue and eigenvector analysis and modal decomposition are used for solving the equations of motion. Controllability analysis shows that although inherently unstable, the lateral disturbance motion is controllable. By feeding back the state variables (i.e. lateral translation velocity, yaw rate, roll rate and roll angle, which can be measured by the sensory system of the insect) to produce anti-symmetrical changes in stroke amplitude and/or in angle of attack between the left and right wings, the motion can be stabilized, explaining why the drone flies can fly stably even if the flight is passively unstable.

Keywords Hovering drone fly · Lateral motion · Flight stability · Stabilization control · Modal analysis

1 Introduction

Flight dynamics (dynamic flight stability and control) is of great importance in the study of biomechanics of insect flight. It also plays a major role in the development of insect-like micro-air vehicles. In recent years, researchers have been devoting more effort to this area (e.g. Refs. [1–5]).

Taylor and Thomas [2] studied dynamic flight stability in the desert locust Schistocerca gregaria at forward flight. Sun and Xiong [3] and Sun et al. [4] studied the dynamic flight stability of several hovering insects. In these studies, an "averaged model" and the linear theory of aircraft flight dynamics were employed, greatly simplifying the analysis (in the averaged model, the wing beat frequency was assumed to be much higher than that of the natural modes of motion of the insect, so that the insect could be treated as a flying body of only six degrees of freedom and the effects of the flapping wings were represented by wing beat-cycle-average aerodynamic and inertial forces and moments that could vary with time over the time scale of the insect body). They showed that for a hovering insect, the longitudinal disturbed motion consisted of an unstable oscillatory mode, a stable fast subsidence mode and a stable slow subsidence mode.

Due to the existence of the unstable mode, the hovering flight of insects is inherently unstable. When the flight of an insect is inherently unstable, the insect must stabilize the flight through adjusting its wing motion constantly. In fact, one of the functions of insect control systems is to provide stability [6]. Deng et al. [5] presented a design of the flight control algorithms for biomimetic robotic insects. Sun and Wang [7] conducted a formal quantitative study on the stabilization control of insect flight based on stability and controllability analysis (controllability is a property of the coupling between the control input and the motion). Sun and Wang's controllability analysis showed that although unstable, the flight was controllable, and that for stable hovering, the unstable oscillatory mode needed to be stabilized and the slow subsidence mode needed stability augmentation, and the former could be accomplished by feeding back pitch attitude, pitch rate and horizontal velocity to produce changes in the mean stroke angle and/or in the angle of attack and the latter by feeding back vertical velocity to produce changes in stroke amplitude and/or in the angle of attack [7].

The project was supported by the National Natural Science Foundation of China (10732030) and the 111 Project (B07009).

Y.-L. Zhang · M. Sun (✉)
Ministry-of-Education Key Laboratory of Fluid Mechanics, Beihang University, 100191 Beijing, China
e-mail: m.sun@263.net

The above works on dynamic stability and stabilization control only investigated the longitudinal motion. Recently, Zhang and Sun [8] studied the lateral dynamic stability of a model insect and showed that the lateral motion was also unstable because of the existence of an unstable divergence mode. Furthermore, the lateral unstable mode diverged faster than the longitudinal unstable mode, showing that the lateral unstable mode would dominate the growth of the disturbance motion. Therefore, it is of great importance to study the stabilization control of lateral motion.

In the present study, we conduct a formal quantitative analysis on the lateral controllability and stabilization control of the hovering flight of a model drone fly, using the techniques based on the linear theories of stability and control. The reason for us to choose the model drone fly is that we have previously studied the lateral stability of the model drone fly [8]. We first used CFD method to compute the flows and obtain the control derivatives (the stability derivatives have been computed in our previous work [8]), and then we used the techniques of eigenvalue and eigenvector analysis and modal decomposition to study the controllability and stabilization control of the insect.

2 Methods

2.1 Equations of motion

The equations of motion have been given in our previous work on lateral stability analysis [8], but the control force terms were not included in the equations since only the stability problem was considered there. Here we give the equations of motion which include the control force terms. Similar to Refs. [2–4, 8], we employ the averaged model: the wing beat frequency of the insect is assumed to be much higher than that of the natural modes of motion of the insect, and the insect is treated as a rigid body of six degrees of freedom, with the action of the flapping wings represented by the wing beat-cycle-average forces and moment. References [4, 9] have shown that the rigid body assumption is applicable to drone flies and many other insects. The model drone fly is sketched in Fig. 1. Let $oxyz$ be a non-inertial coordinate system fixed to the body. The origin o is at the center of mass of the insect body and the axes are aligned so that at equilibrium, the x- and y-axes are horizontal, x-axis points forward and y-axis points to the right of the insect (Fig. 1). It should be noted that although the position of the mass center of the insect's total mass changes with time relative to the body because of the flapping motion of the wings, the position of the mass center of the body does not. The variables that define the lateral motion are the component of velocity along y-axis (denoted as v), the angular-velocity around the x-axis (denoted as p), the angular-velocity around the z-axis (denoted as r), and the angle between the y-axis and the horizontal (denoted as γ).

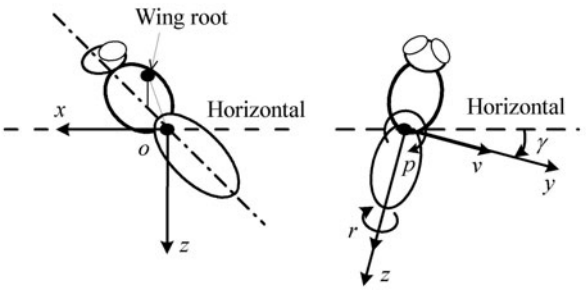

Fig. 1 Definition of the state variables v, p, r and γ and sketches of the reference frames. v, p, r and γ are zero at equilibrium and the model dronefly is shown during a perturbation

The linearized equations of lateral motion are (see Refs. [8, 10])

$$m\delta\dot{v} = \delta Y + g\delta\gamma, \tag{1}$$

$$I_x\delta\dot{p} - I_{xz}\delta\dot{r} = \delta L, \tag{2}$$

$$I_z\delta\dot{r} - I_{xz}\delta\dot{p} = \delta N, \tag{3}$$

$$\delta\dot{\gamma} = \delta p, \tag{4}$$

where m is the mass of the insect (body and wings); g is the gravitational acceleration; I_x and I_z are the moments of inertia about the x- and z-axes, respectively, and I_{xz} is the product of inertia; "˙" represents differentiation with respect to time (t); the symbol δ denotes a small disturbance quantity; Y is the y-component of the mean (wing beat-cycle-average) aerodynamic force, and L and N are mean aerodynamic moments around the x- and z-axes, respectively (the mean inertial forces and moments, including the mean gyroscopic forces and moments, of the wings, are negligible; see Refs. [4, 9]).

Let $\boldsymbol{c}_1$ be the vector of control inputs. It has been observed that freely-flying drone flies and many other insects control the motion mainly by changes in the geometrical angles of attack and changes in the fore/aft extent of the flapping motion [11–14]. Let the geometrical angle of attack in the down stroke translation be denoted as α_{d} and that in the upstroke translation α_{u}; let the stroke amplitude be Φ and the mean stroke angle be $\bar{\phi}$, respectively (α_{d} and α_{u} determine the angle of attack and Φ and $\bar{\phi}$ determine the extent of the fore/aft flapping motion of the wing, see Ref. [8]). On the basis of the observations [11–14], we can assume the following lateral control input vector

$$\boldsymbol{c}_1 = \begin{bmatrix} \delta\Phi_{\mathrm{a}} \\ \delta\alpha_{1\mathrm{a}} \\ \delta\alpha_{2\mathrm{a}} \end{bmatrix}, \tag{5}$$

where the symbol δ denotes a small increment quantity; $\delta\Phi_{\mathrm{a}}$ represents an asymmetrical change in Φ of the left and right wings (e.g. $\delta\Phi_{\mathrm{a}} = 10^\circ$ means that Φ of the left wing increases by 5° and that of the right wing decreases by 5° from

the equilibrium value). $\delta\alpha_{1a}$ represents the following variation in the wing angle of attack: α_d and α_u of the left wing both increase by $|\delta\alpha_{1a}|/2$ and those of the right wing decrease by $|\delta\alpha_{1a}|/2$ from equilibrium values. $\delta\alpha_{2a}$ represents the following variation in the wing angle of attack: for the left wing, α_d increases and α_u decreases by $|\delta\alpha_{2a}|/2$ from their respective equilibrium values; for the right wing, α_d decreases and α_u increases by $|\delta\alpha_{2a}|/2$ from their relative equilibrium values.

The next step of the linearization process is to express the aerodynamic forces and moments as analytical functions of the disturbance motion variables and control inputs. They are represented as (see Ref. [10])

$$\delta Y = Y_v\delta v + Y_p\delta p + Y_r\delta r + Y_{\Phi_a}\delta\Phi_a + Y_{\alpha_{1a}}\delta\alpha_{1a} + Y_{\alpha_{2a}}\delta\alpha_{2a}, \quad (6)$$

$$\delta L = L_v\delta v + L_p\delta p + L_r\delta r + L_{\Phi_a}\delta\Phi_a + L_{\alpha_{1a}}\delta\alpha_{1a} + L_{\alpha_{2a}}\delta\alpha_{2a}, \quad (7)$$

$$\delta N = N_v\delta v + N_p\delta p + N_r\delta r + N_{\Phi_a}\delta\Phi_a + N_{\alpha_{1a}}\delta\alpha_{1a} + N_{\alpha_{2a}}\delta\alpha_{2a}, \quad (8)$$

where Y_v, Y_p, Y_r, L_v, L_p, L_r, N_v, N_p and N_r are lateral stability derivatives, and Y_{Φ_a}, $Y_{\alpha_{1a}}$, $Y_{\alpha_{2a}}$, L_{Φ_a}, $L_{\alpha_{1a}}$, $L_{\alpha_{2a}}$, N_{Φ_a}, $N_{\alpha_{1a}}$ and $N_{\alpha_{2a}}$ are the lateral control derivatives. Substituting Eqs. (6)–(8) into Eqs. (1)–(4), we obtain the linearized equations of lateral motion that include the control force and moment terms

$$\begin{bmatrix} \delta\dot{v}^+ \\ \delta\dot{p}^+ \\ \delta\dot{r}^+ \\ \delta\dot{\gamma} \end{bmatrix} = \boldsymbol{A}_1 \begin{bmatrix} \delta v^+ \\ \delta p^+ \\ \delta r^+ \\ \delta\gamma \end{bmatrix} + \boldsymbol{B}_1 \begin{bmatrix} \delta\Phi_a \\ \delta\alpha_{1a} \\ \delta\alpha_{2a} \end{bmatrix}, \quad (9)$$

where

$$\boldsymbol{A}_1 = \begin{bmatrix} \frac{Y_v^+}{m^+} & \frac{Y_p^+}{m^+} & \frac{Y_r^+}{m^+} & g^+ \\ \frac{I_z^+L_v^+ + I_{xz}^+N_v^+}{I_x^+I_z^+ - I_{xz}^{+2}} & \frac{I_z^+L_p^+ + I_{xz}^+N_p^+}{I_x^+I_z^+ - I_{xz}^{+2}} & \frac{I_z^+L_r^+ + I_{xz}^+N_r^+}{I_x^+I_z^+ - I_{xz}^{+2}} & 0 \\ \frac{I_{xz}^+L_v^+ + I_x^+N_v^+}{I_x^+I_z^+ - I_{xz}^{+2}} & \frac{I_{xz}^+L_p^+ + I_x^+N_p^+}{I_x^+I_z^+ - I_{xz}^{+2}} & \frac{I_{xz}^+L_r^+ + I_x^+N_r^+}{I_x^+I_z^+ - I_{xz}^{+2}} & 0 \\ 0 & 1 & 0 & 0 \end{bmatrix}, \quad (10)$$

$$\boldsymbol{B}_1 = \begin{bmatrix} \frac{Y_{\Phi_a}^+}{m^+} & \frac{Y_{\alpha_{1a}}^+}{m^+} & \frac{Y_{\alpha_{2a}}^+}{m^+} \\ \frac{I_z^+L_{\Phi_a}^+ + I_{xz}^+N_{\Phi_a}^+}{I_x^+I_z^+ - I_{xz}^{+2}} & \frac{I_z^+L_{\alpha_{1a}}^+ + I_{xz}^+N_{\alpha_{1a}}^+}{I_x^+I_z^+ - I_{xz}^{+2}} & \frac{I_z^+L_{\alpha_{2a}}^+ + I_{xz}^+N_{\alpha_{2a}}^+}{I_x^+I_z^+ - I_{xz}^{+2}} \\ \frac{I_{xz}^+L_{\Phi_a}^+ + I_x^+N_{\Phi_a}^+}{I_x^+I_z^+ - I_{xz}^{+2}} & \frac{I_{xz}^+L_{\alpha_{1a}}^+ + I_x^+N_{\alpha_{1a}}^+}{I_x^+I_z^+ - I_{xz}^{+2}} & \frac{I_{xz}^+L_{\alpha_{2a}}^+ + I_x^+N_{\alpha_{2a}}^+}{I_x^+I_z^+ - I_{xz}^{+2}} \\ 0 & 0 & 0 \end{bmatrix}, \quad (11)$$

where the superscript "+" denotes the non-dimensional quantity (in the non-dimensionalization, c, U and t_w are used as the reference length, velocity and time, respectively; here c is the mean chord length of the wing, U is the mean flapping velocity at the radius of the second moment of the wing area (r_2), defined as $U = 2\Phi n r_2$ (Φ is the stroke amplitude and n the stroke frequency) and t_w is the period of the wing beat cycle ($t_w = 1/n$)). The non-dimensional forms are: $m^+ = m/0.5\rho U S_t t_w$ (S_t is the area of two wings), $I_x^+ = I_x/0.5\rho U^2 S_t c t_w^2$, $I_z^+ = I_z/0.5\rho U^2 S_t c t_w^2$, $I_{xz}^+ = I_{xz}/0.5\rho U^2 S_t c t_w^2$ and $g^+ = g t_w/U$; $\delta v^+ = \delta v/U$, $\delta p^+ = \delta p t_w$ and $\delta r^+ = \delta r t_w$; $Y^+ = Y/0.5\rho U^2 S_t$, $L^+ = L/0.5\rho U^2 S_t c$ and $N^+ = N/0.5\rho U^2 S_t c$; $t^+ = t/t_w$. The values of m^+, I_x^+, I_z^+, I_{xz}^+ and g^+ have been computed in Ref. [8] and they are: $m^+ = 92.7$, $I_x^+ = 10.00$, $I_z^+ = 12.69$, $I_{xz}^+ = -8.36$ and $g^+ = 0.015\,8$ (ρ is 1.25 kg/m^3 and g is 9.81 m/s^2).

Note that the equations of motion, Eq. (9), take into account the coupling between the free motion of the insect and the aerodynamic forces and moments acting on the insect, and hence analysis based on these equations is a free-flight analysis.

2.2 Determination of the control derivatives

The equilibrium flight and the stability derivatives have been determined in our previous study on lateral stability analysis using the computational method CFD [8]. Here we only need to compute the control derivatives in the matrix $\boldsymbol{B}_1$. The model wing, the flapping motion, the computational grid and the methods of flow solution and treatment of boundary conditions are the same as those used in the stability study of Ref. [8] and have been described in detail there.

Similar to the calculation of the lateral stability derivatives, conditions in the equilibrium flight are taken as the reference conditions in the calculation of the lateral control derivatives. By definition, a control derivative is a partial derivative, e.g. Y_{Φ_a} represents the rate of change of Y when only $\delta\Phi_a$ is changed from its reference value. In order to obtain the control derivatives, we make 3 consecutive flow computations in which $\delta\Phi_a$, $\delta\alpha_{1a}$ and $\delta\alpha_{2a}$ are varied separately. Using the computed data, curves representing the variation of the aerodynamic forces and moments with each of the 3 control variables are fitted; the partial derivatives are then estimated by taking the local tangent (at equilibrium) of the fitted curves.

2.3 Method of analysis

After the control derivatives are computed (as mentioned above, the stability derivatives are available from Ref. [8]), the elements of the system matrix $\boldsymbol{A}_1$ and control matrix $\boldsymbol{B}_1$ in Eq. (9) become known, and the equation now can be used to study the properties of the disturbance motion of the insect. Here, we are interested in the properties of controllability and the stabilization control of the insect.

Dynamic stability of a system is an inherent property of the system. It deals with the motion of a flying body about its equilibrium state following a disturbance, without active control being applied (it involves the solution of Eq. (9) without the term $\boldsymbol{B}_1\boldsymbol{c}_1$; this has been done in Ref. [8]). The results of stability analysis could show whether or not the system

needs to be controlled. Controllability of a system is a property of the system on the coupling between the control input and the motion (and thus involves the matrices $\boldsymbol{A}_1$ and $\boldsymbol{B}_1$ in Eq. (9)). A linear system is said to be controllable at time t_0 if there exists some input $\boldsymbol{c}(t)$ that makes the disturbance zero at some finite time $t_1(t_1 > t_0)$. The disturbance motion can be represented by a linear combination of the natural modes of motion. Thus knowing the controllability of each of the modes gives the controllability of the flight. For each of the modes, one wishes to know if it is controllable and, if it is, which control inputs are effective for the control. This can be done by using the modal decomposition method. In this method, a linearly dynamic system is transformed into modal coordinates. When the system is in modal coordinates one can immediately see which modes are controlled by which controls. A summary of the modal decomposition method can be found in Bryson [15].

The modal decomposition method is used in the present study to investigate the controllability properties. After the controllability analysis is conducted, the results are used to yield insights into the lateral stabilization control of the insect.

2.4 Flight data

The flight data for the model drone fly has been listed in Ref. [8]. For readers' reference, they are also listed here. The general morphological and kinematic data: body mass m_{bd} is 87.76 mg; the mass of one wing m_{wg} is 0.56 mg; wing length R, 11.2 mm; mean chord length of the wing c is 2.98 mm; radius of second moment of wing area r_2, $0.55R$; the radial distance between the wing-root to the center of mass of the wing $r_{1,\mathrm{m}}$, $0.35R$; area of one wing S, 33.34 mm^2; body length l_{b}, 14.11 mm; distance between two wing roots, $0.33\,l_{\mathrm{b}}$; distance from the wing base axis to the center of mass l_{l}, $0.13\,l_{\mathrm{b}}$; free body angle χ_0, 52° (note that l_{l} and χ_0 determine the relative position of the center of mass and the wing roots [14], which is needed in the calculation of the aerodynamic moment about the center of mass); $I_x = 657.7\,\mathrm{mg{\cdot}mm^2}$, $I_y = 1\,308.5\,\mathrm{mg{\cdot}mm^2}$, $I_z = 834.6\,\mathrm{mg{\cdot}mm^2}$ and $I_{xz} = -550.0\,\mathrm{mg{\cdot}mm^2}$; $\Phi = 107.1°$; $n = 164$ Hz; Δt_{r} is 30% of wing beat cycle; the stroke plane angle is assumed to be horizontal; body angle χ is 42°; the Reynolds number of a wing Re, which is needed in the non-dimensionalized Navier-Stokes equations, is 781.6 (Re is defined as $Re = cU/\nu$, where ν is the kinematic viscosity of the air).

3 Results and discussion

3.1 Control derivatives

Using the method described in Sect. 2.2, the control derivative is calculated. Flows for each of the control variables varying independently from the equilibrium value are computed. The corresponding Y^+, L^+ and N^+ values are obtained. The Φ_{a}-series, $\alpha_{1\mathrm{a}}$-series and $\alpha_{2\mathrm{a}}$-series data are plotted in Fig. 2. It is observed that Y^+, L^+ and N^+ vary approxi-

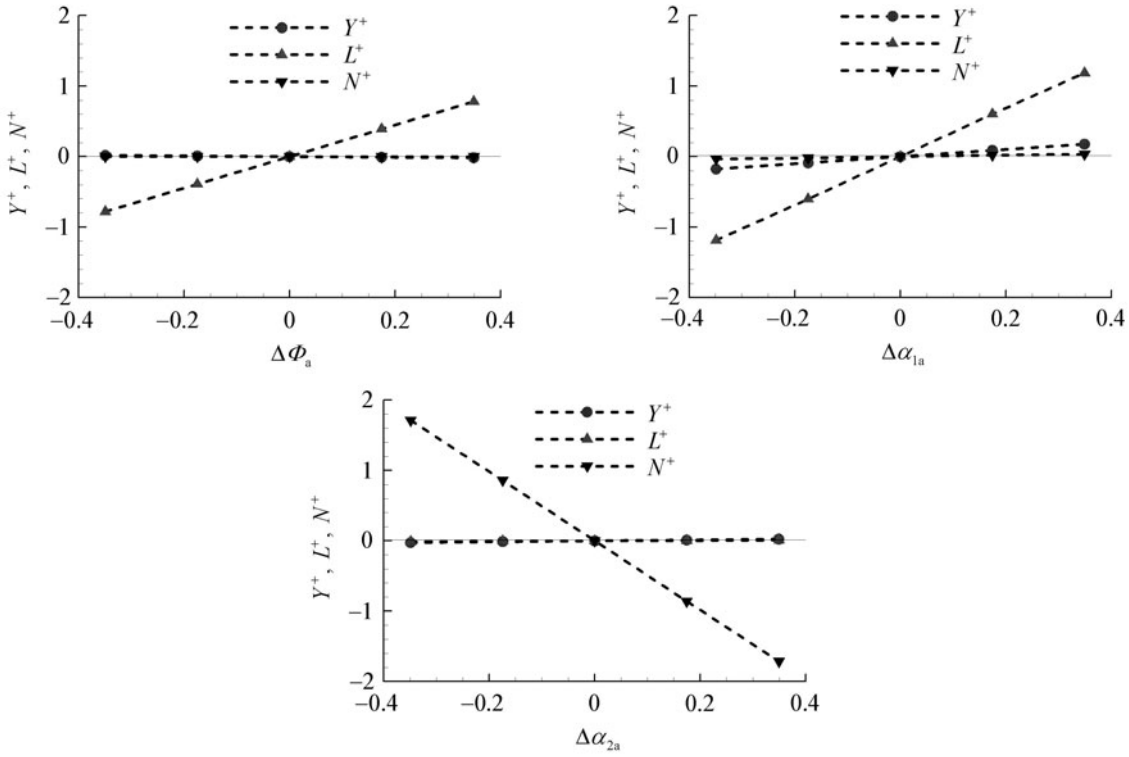

Fig. 2 The Φ_{a}-series, $\alpha_{1\mathrm{a}}$-series and $\alpha_{2\mathrm{a}}$-series force and moment data

mately linearly with $\Delta\Phi_a$, $\Delta\alpha_{1a}$ and $\Delta\alpha_{2a}$ in a range of $-0.4 \le \Delta\Phi_a$, $\Delta\alpha_{1a}$ and $\Delta\alpha_{2a} \le 0.4$, showing that the linear model is justified for small variations in control variables. The control derivatives, estimated using these data, are shown in Table 1. From Table 1, it is seen that varying Φ_a or α_{1a} mainly produces a change in roll moment ($L^+_{\Phi_a}$ is much larger than the other Φ_a-derivatives and $L^+_{\alpha_{1a}}$ is much larger than the other α_{1a}-derivatives) and varying α_{2a} mainly produces a change in yaw moment ($N^+_{\alpha_{2a}}$ is much larger than other α_{2a}-derivatives).

Table 1 Non-dimensional control derivatives

$Y^+_{\Phi_a}$	$L^+_{\Phi_a}$	$N^+_{\Phi_a}$	$Y^+_{\alpha_{1a}}$	$L^+_{\alpha_{1a}}$	$N^+_{\alpha_{1a}}$	$Y^+_{\alpha_{2a}}$	$L^+_{\alpha_{2a}}$	$N^+_{\alpha_{2a}}$
−0.049	2.236	−0.007	0.511	3.456	0.121	0.066	0.014	−4.922

3.2 How the control derivatives are produced

The stabilization control properties are closely related to the control derivatives and it is of great interest to examine how they are produced.

First, we consider the derivatives with respect to Φ_a. As see in Table 1, the magnitude of L_{Φ_a} is relatively large and Y_{Φ_a} and N_{Φ_a} are almost zero. When $\Delta\Phi_a$ is positive, i.e. Φ of the left wing being increased and that of the right wing decreased, the translation velocity (proportional to $\Phi n r_2$) of the left wing is increased and that of the right wing decreased relative to the value of equilibrium flight. Thus, the lift and drag of the left wing will be increased and those of the right wing decreased. The lift of a wing is perpendicular to the stroke plane (note that the stroke plane is parallel to the x-y plane of the reference frame). As seen from Fig. 3, the difference in the mean lift between the left and right wings will produce a rolling moment. Since the distance between the action lines of these two mean lift forces are relatively large (one is at the outer part of the left wing and the other at the outer part of the right wing, see Fig. 3), the rolling moment can be large, explaining the large L_{Φ_a} derivative.

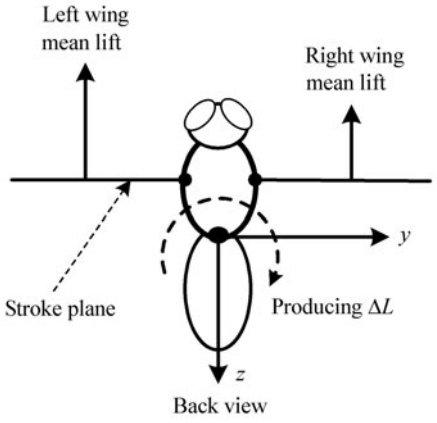

Fig. 3 Mean lift forces of the left and right wings when $\Delta\Phi_a > 0$

The drag of a wing is in the stroke plane and it mainly produces side force and yaw moment. Focusing on the drag force of the left wing, as seen from Fig. 4, in the downstroke (Fig. 4a), the y-component of drag in the first half of the downstroke is opposite to that in the second half of the downstroke; the x-component of drag is in the negative x-direction in the whole downstroke. Thus the downstroke will produce a net force in a negative x-direction and produce little net side force. For the upstroke (Fig. 4b), similar analysis shows that a net force in the positive x-direction will be produced and little side force produced. In one whole wing beat cycle, the force in the negative x-direction in the downstroke will be approximately canceled by the force in the positive x-direction in the upstroke. As a result, the left wing produces little mean force in the stroke plane. It can be shown that this is also true for the right wing. This explains why Y_{Φ_a} and N_{Φ_a} are very small.

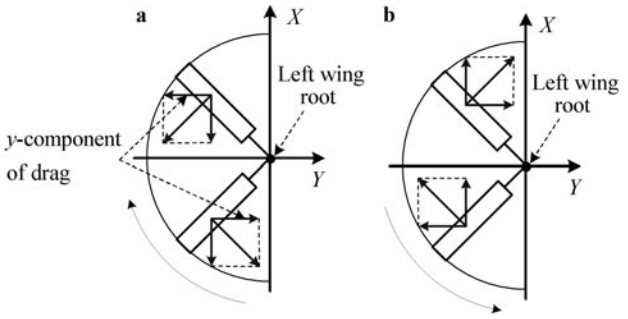

Fig. 4 Drag force of the left wing and its y- and x-components (X and Y axes are parallel to x and y axes, respectively). **a** Downstroke; **b** Upstroke

Next, we examine the derivatives with respect to α_{2a}. As aforementioned, $\Delta\alpha_{2a}$ mainly produces a yaw moment derivative ($N_{\alpha_{2a}}$) and the side force and roll moment derivatives ($Y_{\alpha_{2a}}$ and $L_{\alpha_{2a}}$) produced are very small (see Table 1). When $\Delta\alpha_{2a}$ is positive, the left-wing down stroke angle of attack (α_d) is increased and the upstroke angle of attack (α_u) decreased relative to the value of equilibrium flight; for the right wing, the variation of angle of attack is opposite to that of the left wing. Let's first look at the left wing. During the down stroke, the lift and drag are increased because α_d is increased, and during the upstroke they are decreased be-

cause α_u is decreased. Thus, the mean lift in a wing beat cycle will not change much relative to the value of equilibrium flight. As seen from Fig. 5, the x-component of the drag in the down stroke (Fig. 5a) is in the negative x-direction and has a relatively large magnitude because α_d is increased, and the x-component of the drag in the upstroke (Fig. 5b) is in the positive x-direction and has a relatively small magnitude because α_u is decreased (as discussed above, the drag has little net y-component force in a down stroke or upstroke). Thus, in a whole cycle, the left wing drag will give a mean force in the negative x-direction. For the right wing, it can be similarly shown that the wing beat-cycle-mean lift will not change much from the value of equilibrium flight but the drag will give a mean force in the positive x-direction. Since both the left and right wings do not produce any change in mean lift, little roll moment can be produced and since both the left and right wings produce little net y-component force, little side force can be produced, explaining the very small L and Y derivatives. The mean force in the negative x-direction produced by the left wing and the mean force in the positive x-direction produced by the right wing will give a yaw moment; since the distance between the action lines of these two forces is large (one is at the outer part of the left wing and the other at the outer part of the right wing), the yaw moment can be relatively large, explaining the large $N_{\alpha_{2a}}$ derivative.

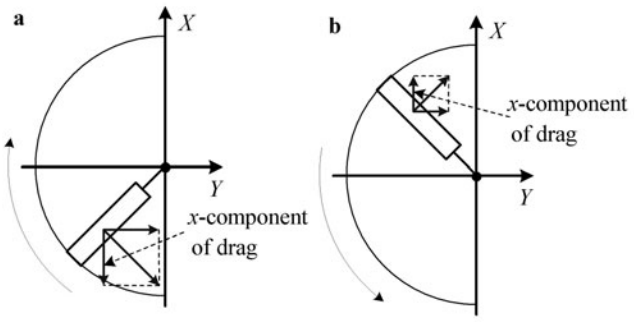

Fig. 5 Drag force of the left wing and its x- and y-components (X and Y axes are parallel to x and y axes, respectively). **a** Downstroke; **b** Upstroke

The explanation of the derivatives with respect to α_{1a} is similar to that with respect to Φ_a.

3.3 Controllability analysis

The stability derivatives are available from Ref. [8]. Now the control derivatives have been computed. Hence the elements of the system matrix $\boldsymbol{A}_l$ and the control matrix $\boldsymbol{B}_l$ in Eq. (9) become known. They are

$$\boldsymbol{A}_l = \begin{bmatrix} -0.009\,4 & -0.001\,1 & 0 & 0.015\,8 \\ 0.174\,1 & -0.249\,6 & 0.293\,0 & 0 \\ -0.111\,7 & 0.155\,1 & -0.350\,0 & 0 \\ 0 & 1 & 0 & 0 \end{bmatrix}, \quad (12)$$

$$\boldsymbol{B}_l = \begin{bmatrix} -0.000\,5 & 0.005\,5 & 0.000\,7 \\ 0.499\,3 & 0.752\,6 & 0.726\,0 \\ -0.329\,6 & -0.486\,4 & -0.866\,4 \\ 0 & 0 & 0 \end{bmatrix}. \quad (13)$$

As mentioned above, the lateral stability properties of the disturbance motion of the drone fly have been studied by the present authors [8]; for reference, the eigenvalues of $\boldsymbol{A}_l$ (denoted as λ_1, $\lambda_{2,3}$ and λ_4) and the corresponding eigenvectors computed in Ref. [8] are given in Tables 2 and 3, respectively. They represent an unstable slow divergence mode, a stable slow oscillatory mode and a stable fast subsidence mode, respectively (see Ref. [8]). Because of the existence of the unstable mode, the lateral motion of the insect is inherently unstable (not having passive stability).

Table 2 Eigenvalues of the system matrix $\boldsymbol{A}_l$

Mode 1	Mode 2	Mode 3
λ_1	$\lambda_{2,3}$	λ_4
0.079	-0.089 ± 0.057i	-0.510

Table 3 Eigenvectors of the system matrix $\boldsymbol{A}_l$

	Mode 1	Mode 2	Mode 3
δv^+	0.179 (0°)	0.163 (−144.7°)	0.033 (180°)
δp^+	0.079 (0°)	0.106 (147.5°)	0.510 (180°)
δr^+	0.018 (180°)	0.072 (74.6°)	0.472 (0°)
$\delta\gamma$	1 (0°)	1 (0°)	1 (0°)

Drone flies are observed to fly stably. Here we use Eq. (9) to study the flight controllability of the model drone fly and try to explain why the drone flies can fly stably, even though they do not have passive stability. We apply the modal decomposition method [15] to the system. Let $\boldsymbol{M}_l$ denote the eigenvector matrix of $\boldsymbol{A}_l$

$$\boldsymbol{M}_l = \begin{bmatrix} \boldsymbol{\eta}_1 & 2\boldsymbol{\eta}_2 & 2\boldsymbol{\eta}_3 & \boldsymbol{\eta}_4 \end{bmatrix}, \quad (14)$$

where $\boldsymbol{\eta}_1$, $\boldsymbol{\eta}_2 \pm \boldsymbol{\eta}_3$i and $\boldsymbol{\eta}_4$ are the eigenvectors corresponding to λ_1, $\lambda_{2,3}$ and λ_4. Let

$$\begin{bmatrix} \delta v^+ \\ \delta p^+ \\ \delta r^+ \\ \delta\gamma \end{bmatrix} = \boldsymbol{M}_l \begin{bmatrix} \xi_1 \\ \xi_2 \\ \xi_3 \\ \xi_4 \end{bmatrix}, \quad (15)$$

where ξ_1, ξ_2, ξ_3 and ξ_4 are the modal coordinates. Substituting Eq. (15) into Eq. (9), and then multiplying the two sides of the resulting equation by $\boldsymbol{M}_1^{-1}$, we obtain

$$\begin{bmatrix} \dot{\xi}_1 \\ \dot{\xi}_2 \\ \dot{\xi}_3 \\ \dot{\xi}_4 \end{bmatrix} = \boldsymbol{A}_{\mathrm{lnn}} \begin{bmatrix} \xi_1 \\ \xi_2 \\ \xi_3 \\ \xi_4 \end{bmatrix} + \boldsymbol{B}_{\mathrm{ln}} \begin{bmatrix} \delta\Phi_{\mathrm{a}} \\ \delta\alpha_{1\mathrm{a}} \\ \delta\alpha_{2\mathrm{a}} \end{bmatrix}, \tag{16}$$

where

$$\boldsymbol{A}_{\mathrm{lnn}} = \boldsymbol{M}_1^{-1}\boldsymbol{A}_1\boldsymbol{M}_1, \tag{17}$$

$$\boldsymbol{B}_{\mathrm{ln}} = \boldsymbol{M}_1^{-1}\boldsymbol{B}_1. \tag{18}$$

Equations (16)–(18) are the modal form of Eq. (9). Once the system is in modal form, one can immediately see which modes are controllable and can be controlled by which control inputs. $\boldsymbol{A}_{\mathrm{lnn}}$ and $\boldsymbol{B}_{\mathrm{ln}}$ in the model form are computed and the results are given below

$$\boldsymbol{A}_{\mathrm{lnn}} = \begin{bmatrix} 0.078\,6 & 0 & 0 & 0 \\ 0 & -0.089\,0 & 0.056\,8 & 0 \\ 0 & -0.056\,8 & -0.089\,0 & 0 \\ 0 & 0 & 0 & -0.509\,7 \end{bmatrix}, \tag{19}$$

$$\boldsymbol{B}_{\mathrm{ln}} = \begin{bmatrix} -0.571\,1 & -0.890\,1 & -0.280\,9 \\ 0.138\,7 & 0.185\,1 & 0.749\,8 \\ 0.497\,9 & 0.774\,7 & -0.485\,9 \\ -1.013\,5 & -1.505\,6 & -2.124\,3 \end{bmatrix}. \tag{20}$$

From $\boldsymbol{A}_{\mathrm{lnn}}$, we see that ξ_1 is the modal coordinate of the unstable slow divergence mode, ξ_2 and ξ_3 are the modal coordinates of the stable slow oscillatory mode and ξ_4 is the modal coordinate of the stable fast subsidence mode. For stable flight, the unstable mode needs to be stabilized, and one of the stable modes, the slow oscillatory mode, needs stability augmentation (the magnitude of the real part of $\lambda_{2,3}$ is 0.089, relatively small; i.e. although stable, this mode converges very slowly: it needs a period of about 7 wing beats for the initial disturbance to decrease to half its initial value). Examining Eqs. (16) and (20), we see that the unstable mode (ξ_1) and the slow stable mode (ξ_2 and ξ_3) are well controlled by $\delta\Phi_{\mathrm{a}}$ and/or $\delta\alpha_{1\mathrm{a}}$ and/or $\delta\alpha_{2\mathrm{a}}$ (the magnitude of all the elements in $\boldsymbol{B}_{\mathrm{ln}}$ are not small).

The above results show that the flight is controllable. This may explain why drone flies can fly stably, even if they do not have passive stability.

3.4 Stabilization control

Here we consider an example to which the above theory is applied and conceptually study the possible ways the model insect may stabilize its hovering flight. As shown above, the unstable mode is well controlled by $\delta\Phi_{\mathrm{a}}$ and/or $\delta\alpha_{1\mathrm{a}}$ and/or $\delta\alpha_{2\mathrm{a}}$. We consider the case of $\delta\Phi_{\mathrm{a}}$ being used to stabilize the motion. In this case, Eq. (9) can be written as

$$\begin{bmatrix} \delta\dot{v}^+ \\ \delta\dot{p}^+ \\ \delta\dot{r}^+ \\ \delta\dot{\gamma} \end{bmatrix} = \begin{bmatrix} \frac{Y_v^+}{m^+} & \frac{Y_p^+}{m^+} & \frac{Y_r^+}{m^+} & g^+ \\ \frac{I_z^+L_v^+ + I_{xz}^+N_v^+}{I_x^+I_z^+ - I_{xz}^{+2}} & \frac{I_z^+L_p^+ + I_{xz}^+N_p^+}{I_x^+I_z^+ - I_{xz}^{+2}} & \frac{I_z^+L_r^+ + I_{xz}^+N_r^+}{I_x^+I_z^+ - I_{xz}^{+2}} & 0 \\ \frac{I_{xz}^+L_v^+ + I_x^+N_v^+}{I_x^+I_z^+ - I_{xz}^{+2}} & \frac{I_{xz}^+L_p^+ + I_x^+N_p^+}{I_x^+I_z^+ - I_{xz}^{+2}} & \frac{I_{xz}^+L_r^+ + I_x^+N_r^+}{I_x^+I_z^+ - I_{xz}^{+2}} & 0 \\ 0 & 1 & 0 & 0 \end{bmatrix} \times \begin{bmatrix} \delta v^+ \\ \delta p^+ \\ \delta r^+ \\ \delta\gamma \end{bmatrix} + \begin{bmatrix} \frac{Y_{\Phi_{\mathrm{a}}}^+}{m^+} \\ \frac{I_z^+L_{\Phi_{\mathrm{a}}}^+ + I_{xz}^+N_{\Phi_{\mathrm{a}}}^+}{I_x^+I_z^+ - I_{xz}^{+2}} \\ \frac{I_{xz}^+L_{\Phi_{\mathrm{a}}}^+ + I_x^+N_{\Phi_{\mathrm{a}}}^+}{I_x^+I_z^+ - I_{xz}^{+2}} \\ 0 \end{bmatrix} \delta\Phi_{\mathrm{a}}. \tag{21}$$

Drone flies and many other insects can measure the lateral velocity and body rotation rates using their compound eyes and antennae [6]; the roll angle information could be obtained by integration of the roll rate. Therefore, it is reasonable to assume that drone flies can feed back all the state variables, δv^+, δp^+, δr^+ and $\delta\gamma$, to produce the control input $\delta\Phi_{\mathrm{a}}$, i.e.

$$\delta\Phi_{\mathrm{a}} = \begin{bmatrix} k_1 & k_2 & k_3 & k_4 \end{bmatrix} \begin{bmatrix} \delta v^+ \\ \delta p^+ \\ \delta r^+ \\ \delta\gamma \end{bmatrix}. \tag{22}$$

Substituting Eq. (22) into Eq. (21) gives

$$\begin{bmatrix} \delta\dot{v}^+ \\ \delta\dot{p}^+ \\ \delta\dot{r}^+ \\ \delta\dot{\gamma} \end{bmatrix} = \boldsymbol{A}_1' \begin{bmatrix} \delta v^+ \\ \delta p^+ \\ \delta r^+ \\ \delta\gamma \end{bmatrix}, \tag{23}$$

where

$$\boldsymbol{A}_1' = \begin{bmatrix} -0.009\,4 & -0.001\,1 & 0 & 0.015\,8 \\ 0.174\,1 & -0.249\,6 & 0.293\,0 & 0 \\ -0.111\,7 & 0.155\,1 & -0.350\,0 & 0 \\ 0 & 1 & 0 & 0 \end{bmatrix}$$

$$+\begin{bmatrix} -0.000\,5 \\ 0.499\,3 \\ -0.329\,6 \\ 0 \end{bmatrix}\begin{bmatrix} k_1 & k_2 & k_3 & k_4 \end{bmatrix}. \tag{24}$$

The characteristic equation of matrix $\boldsymbol{A}_1'$ is

$$\lambda^4 + b\lambda^3 + c\lambda^2 + d\lambda + e = 0, \tag{25}$$

where

$$b = 0.609 + 5\times10^{-4}k_1 - 0.499\,3k_2 + 0.329\,6k_3, \tag{26a}$$

$$c = 4.774\times10^{-2} + 8.49\times10^{-4}k_1 - 8.278\,9\times10^{-2}k_2 + 7.869\,1\times10^{-3}k_3 - 0.499\,3k_4, \tag{26b}$$

$$d = -2.325\,7\times10^{-3} - 7.782\times10^{-3}k_1 - 7.208\,1\times10^{-4}k_2 + 4.671\times10^{-5}k_3 - 8.279\times10^{-3}k_4, \tag{26c}$$

$$e = 4.456\,7\times10^{-4} - 1.235\,3\times10^{-3}k_1 - 2.546\,2\times10^{-5}k_3 - 7.208\,1\times10^{-4}k_4. \tag{26d}$$

Equation (25) is a quartic equation and analytical expressions expressing its roots (eigenvalues λ_1, $\lambda_{2,3}$ and λ_4) in terms of k_1, k_2, k_3 and k_4 can be obtained. In principle, given the desired eigenvalues, the values of k_1, k_2, k_3 and k_4 can be determined using these expressions. In practice, it is difficult to do this because for a quartic equation, these expressions are very complex. However, since the roots are known, the coefficients of Eq. (25), i.e. b, c, d and e, can be computed using the relations between coefficients and roots

$$\sum_{i=1}^{4}\lambda_i = -b, \qquad \sum_{i,j=1(i<j)}^{4}\lambda_i\lambda_j = c,$$

$$\sum_{i,j,k=1(i<j<k)}^{4}\lambda_i\lambda_j\lambda_k = -d, \qquad \prod_{i=1}^{4}\lambda_i = e,$$

and k_1, k_2, k_3 and k_4 can be easily determined by solving a set of 4 linear equations (i.e. Eqs. (26a) and (26b). Suppose it is desired that $\lambda_1 = 0.0$ and the other eigenvalues remain the same, so that the flight is neutrally stable. With b, c, d and e computed using these values of λ_1, $\lambda_{2,3}$ and λ_4, solving Eqs. (26a) and (26b) gives

$$k_1 = -0.319\,2, \qquad k_2 = -0.287\,9,$$

$$k_3 = -0.196\,9, \qquad k_4 = -0.064\,3.$$

This shows that if the model insect uses the following controls

$$\delta\Phi_\mathrm{a} = -0.319\,2\delta v^+ - 0.287\,9\delta p^+ - 0.196\,9\delta r^+ - 0.064\,3\delta\gamma, \tag{27}$$

the lateral motion could become neutrally stable. (Similarly, it can be shown that the lateral motion could be stabilized using $\delta\alpha_{1\mathrm{a}}$ or $\delta\alpha_{2\mathrm{a}}$ controls.)

An interesting point shown by the above results is that only very small $\delta\Phi_\mathrm{a}$, or a very small difference in stroke amplitude between the left and right wings, is needed for lateral stabilization control. This can be seen from Eq. (27) and the eigenvectors in Table 3. Suppose that in the disturbance motion, $\delta\gamma$ is 0.5, that is, the insect rolls by about 30°. From the eigenvector of the unstable mode (Mode 1, in Table 3), we see that δv^+, δp^+ and δr^+ would be about 0.05 or less. Then, from Eq. (27), the magnitude of $\delta\Phi_\mathrm{a}$ would be around 0.05, only a few degrees.

3.5 The longitudinal motion

The above analysis is on the stabilization control properties of the lateral disturbance motion. As mentioned above, the disturbed flight of an insect includes both the longitudinal and lateral motions. The longitudinal stability and stabilization control of hovering insects have been studied by our group [7, 16]. For readers' reference, we include the longitudinal stabilization control properties of the present model drone fly here.

The longitudinal aerodynamic and control derivatives of the present model drone fly have been calculated by Wu and Sun in a previous study [17], and the longitudinal system matrix ($\boldsymbol{A}$) and control matrix ($\boldsymbol{B}$) are (see Ref. [17])

$$\boldsymbol{A} = \begin{bmatrix} -0.013\,4 & 0.001\,1 & -0.002\,5 & -0.015\,8 \\ -0.000\,6 & -0.012\,2 & -0.000\,3 & 0 \\ 0.089\,5 & -0.006\,2 & -0.009\,8 & 0 \\ 0 & 0 & 1 & 0 \end{bmatrix}, \tag{28}$$

$$\boldsymbol{B} = \begin{bmatrix} 0 & 0.000\,9 & -0.002\,2 & -0.032\,1 \\ -0.018\,0 & -0.026\,6 & 0 & -0.000\,1 \\ 0.001\,1 & 0.001\,3 & -0.155\,6 & 0.024\,7 \\ 0 & 0 & 0 & 0 \end{bmatrix}. \tag{29}$$

The longitudinal control variables or control inputs are $\delta\Phi$, $\delta\bar{\phi}$, $\delta\alpha_1$ and $\delta\alpha_2$ ($\delta\Phi$ and $\delta\bar{\phi}$ represent changes in stroke amplitude and mean stroke angle, respectively; $\delta\alpha_1$ represents an equal change whilst $\delta\alpha_2$ represents a differential change in the geometrical angles of attack of the down stroke and upstroke; see Ref. [17]).

The modal form of the longitudinal equations of motion is

$$\begin{bmatrix} \dot{\xi}_1 \\ \dot{\xi}_2 \\ \dot{\xi}_3 \\ \dot{\xi}_4 \end{bmatrix} = \boldsymbol{A}_\mathrm{nn}\begin{bmatrix} \xi_1 \\ \xi_2 \\ \xi_3 \\ \xi_4 \end{bmatrix} + \boldsymbol{B}_\mathrm{n}\begin{bmatrix} \delta\Phi \\ \delta\alpha_1 \\ \delta\bar{\phi} \\ \delta\alpha_2 \end{bmatrix}, \tag{30}$$

where ξ_1, ξ_2, ξ_3 and ξ_4 are the modal coordinates, and

$$\boldsymbol{A}_{\mathrm{nn}} = \begin{bmatrix} 0.048\,1 & -0.097\,7 & 0 & 0 \\ 0.097\,7 & 0.048\,1 & 0 & 0 \\ 0 & 0 & -0.119\,5 & 0 \\ 0 & 0 & 0 & -0.012\,3 \end{bmatrix}, \quad (31)$$

$$\boldsymbol{B}_{\mathrm{n}} = \begin{bmatrix} 0.000\,4 & -0.000\,8 & -0.220\,1 & 0.074\,2 \\ 0.005\,5 & 0.009\,2 & -0.431\,2 & 0.001\,2 \\ 0.000\,5 & 0.003\,4 & 0.441\,3 & -0.148\,8 \\ -0.018\,1 & -0.026\,7 & -0.001\,1 & 0 \end{bmatrix}. \quad (32)$$

Equations (30) and (31) show that similar to the results in the previous study [7, 16], the longitudinal disturbance motion has an unstable oscillatory mode (ξ_1 and ξ_2), a stable fast subsidence mode (ξ_3) and a stable slow subsidence mode (ξ_4).

Equations (30) and (32) show that, also similar to the results in the previous study [7, 16], the unstable oscillatory mode (ξ_1 and ξ_2) is well controlled by $\delta\bar{\phi}$ and/or $\delta\alpha_2$ and the stable slow subsidence mode (ξ_4) is well controlled by $\delta\Phi$ and/or $\delta\alpha_1$.

We thus see that for the present model drone fly, both the lateral and longitudinal disturbance motions are controllable, and that the unstable modes and the slow stable modes could be stabilized or improved by changes in longitudinal control inputs $\delta\Phi$, $\delta\bar{\phi}$, $\delta\alpha_1$ and $\delta\alpha_2$ and lateral control inputs $\delta\Phi_{\mathrm{a}}$, $\delta\alpha_{1\mathrm{a}}$ and $\delta\alpha_{2\mathrm{a}}$.

3.6 Some discussion on the linear analysis

The above results are based on the linearized stability and control analysis. Here, we discuss the range of applicability of the above results. When linearizing the equations of motion to obtain the linear system equation (9), we have assumed that the aerodynamic forces and moments, Y, L and N, vary approximately linearly with the state variables (δv^+, δp^+ and δr^+) and control variables ($\delta\Phi_{\mathrm{a}}$, $\delta\alpha_{1\mathrm{a}}$ and $\delta\alpha_{2\mathrm{a}}$) and that $\delta\gamma^3$, $\delta r^+\delta u^+$, $\delta p^+\delta w^+$, $\delta q^+\delta r^+$, $\delta p^+\delta q^+$, etc., are negligibly small compared with the first-order terms.

First, let's look at the linearity of Y, L and N. From Fig. 2 (and Fig. 5 of Ref. [8]), it is observed that when $-0.15 \le \delta v^+$, δp^+ and $\delta r^+ \le 0.15$ and $-0.4 \le \Delta\Phi_{\mathrm{a}}, \Delta\alpha_{1\mathrm{a}}$ and $\Delta\alpha_{2\mathrm{a}} \le 0.4$, the linearity of Y, L and N are generally good. Thus, for the assumption of Y, L and N varying linearly with the state and control variables to be reasonable, the state and control variable should be in the range of $-0.15 \le \delta v^+$, δp^+ and $\delta r^+ \le 0.15$ and $-0.4 \le \Delta\Phi_{\mathrm{a}}, \Delta\alpha_{1\mathrm{a}}$ and $\Delta\alpha_{2\mathrm{a}} \le 0.4$.

Next, we look at the assumption of $\delta\gamma^3$, $\delta r^+\delta u^+$, $\delta p^+\delta w^+$, $\delta q^+\delta r^+$ and $\delta p^+\delta q^+$ being much smaller than the first order terms. If δr^+, δu^+, δp^+, δw^+ and δq^+ are less than 0.15, $\delta r^+\delta u^+$, $\delta p^+\delta w^+$, $\delta q^+\delta r^+$ and $\delta p^+\delta q^+$ are clearly smaller by one order of magnitude than the first order terms (the first order terms are of order 0.1). As for $\delta\gamma^3$, even if $\delta\gamma$ is 0.22 (about 13 degrees), $\delta\gamma^3$ (= 0.01) is still of higher order small.

From the above, it can be said that when the state variables are in the range of $-0.15 \le \delta v^+$, δp^+ and $\delta r^+ \le 0.15$ and $-0.22 \le \delta\gamma \le 0.22$ and the control variables are in the range of $-0.4 \le \Delta\Phi_{\mathrm{a}}, \Delta\alpha_{1\mathrm{a}}$ and $\Delta\alpha_{2\mathrm{a}} \le 0.4$, the linear theory could give reasonably good results (of course, when the state variables and control variables are larger, the linear theory may have errors in its prediction).

The above ranges are not very restrictive: e.g. δv can be as large as $0.15U$ and $\delta\gamma$ can be as large as 0.22 radians (13 degrees). These values are not very small. Furthermore, it is expected that for an insect who wishes to hover at a fixed point in the air, disturbances will be suppressed before they grow large. Therefore, it is believed that the present analysis of insect stabilization control has reasonable accuracy.

4 Conclusion

In this study, we investigate the lateral stabilization control of the model drone fly. The method of computational fluid dynamics is used to compute the lateral control derivatives and the techniques of eigenvalue and eigenvector analysis and modal decomposition are used for solving the equations of motion. Controllability analysis shows that although inherently unstable, the lateral disturbance motion is controllable. By feeding back the state variables (i.e. lateral translation velocity, yaw rate, roll rate and roll angle, which can be measured by the sensory system of the insect) to produce anti-symmetrical changes in stroke amplitude and/or in the angle of attack between the left and right wings, the motion can be stabilized, explaining why drone flies can fly stably even if the flight is passively unstable.

References

1 Taylor, G.K., Thomas, A.L.R.: Animal flight dynamics. II. Longitudinal stability in flapping flight. J. Theor. Biol. **214**, 351–370 (2002)

2 Taylor, G.K., Thomas, A.L.R.: Dynamic flight stability in the desert locust Schistocerca gregaria, J. Exp. Biol. **206**, 2803–2829 (2003)

3 Sun, M., Xiong, Y.: Dynamic flight stability of a hovering bumblebee, J. Exp. Biol. **208**, 447–459 (2005)

4 Sun, M., Wang, J.K., Xiong Y.: Dynamic flight stability of hovering insects. Acta Mech. Sin. **208**, 447–459 (2007)

5 Deng, X., Schenato, L., Sadtry, S.S.: Flapping flight for biomimetic robotic insects: part II, flight control design. IEEE Transactions on Robotics **22**, 789–803 (2006)

6 Dudley, R.: The Biomechanics of Insect Flight: Form, Function, Evolution. Princeton University Press, Princeton (2000)

7 Sun, M., Wang, J.K.: Flight stabilization control of a hovering model insect. J. Exp. Biol. **210**, 2714–2722 (2007)

8 Zhang, Y.L., Sun, M.: Dynamic flight stability of a hovering model insect: lateral motion. Acta Mech. Sin. **26**, 175–190

(2010)
9 Zhang, Y.L., Sun, M.: Dynamic flight stability of hovering model insects: theory vs. simulation using equations of motion coupled with Navier-Stokes equations. Acta Mech. Sin. **26**, 509–520 (2010)
10 Etkin, B., Reid, L.D.: Dynamics of Atmospheric Flight. John Wiley and Sons, Inc. New York (1996)
11 Ellington, C.P.: The aerodynamics of hovering insect flight. III. Kinematics. Phil. Trans. R. Soc. Lond. B **305**, 79–113 (1984)
12 Ennos, A.R.: The kinematics and aerodynamics of the free flight of some Diptera, J. Exp. Biol. **142**, 49–85 (1989)
13 Zhang, Y.L., Sun, M.: Dynamic flight stability and control of a hovering model dronefly: experiment, theory and numerical simulation. [Ph.D. Thesis], Beijing University of Aeronautics and Astronautics, Department of Aeronautical Engineering (2010)
14 Zhang, Y.L., Sun, M.: Wing kinematics measurement and aerodynamics of free-flight maneuvers in drone-flies. Acta Mech. Sin. **26**, 371–382 (2010)
15 Bryson A. E.: Control of Spacecraft and Aircraft. Princeton University Press, Princeton (1994)
16 Xiong, Y., Sun, M.: Stabilization control of a bumblebee in hovering and foreward flight. Acta Mech. Sin. **25**, 13–21 (2009)
17 Wu J.H., Sun, M.: Control for going from hovering to small speed flight of a model insect. Acta Mech. Sin. **25**, 295–302 (2009)